A Programmable Soft Chemo-mechanical Actuator Exploiting a Catalyzed Photochemical Water-Oxidation Reaction

P. Yuan,[1] J. M. McCracken,[1] D. E. Gross,[1] P. V. Braun,[2] J. S. Moore,[1] and R. G. Nuzzo[1†]

[1]*School of Chemical Sciences, University of Illinois at Urbana-Champaign, Urbana, Illinois 61801 (USA)*

[2] *Materials Science and Engineering, University of Illinois at Urbana-Champaign, Urbana, IL 61801 (USA)*

[†]*corresponding author contact information: r-nuzzo@gmail.com*

Table of Contents

S1. Synthesis of RuIrPAA Composites S2

S2. Underlying Polymer Chemistry and Molding Methods S3

S3. Molding-Based Fabrication of Polymer Actuators S5

S4. Quantification of IrO_2 Hydrogel Absorption S6

S5. Experimental Controls and Procedures S8

S6. Bimorph Composition and Solution Conditions at pH 5.5 ..... S10

S7. Mechanisms of Single Cycle System Reversibility for Bimorph Composite S12

S8. Catalytically-Induced Proton Gradients S13

S9. Mechanisms of Multi-Cycle Reversibility S14

S10. Mechanical Bending of Bimorph System S15

S11. Reaction Efficiency S17

S12. References S17

S.1 Synthesis of RuIrPAA Composites

S1.1. Methacrylate-Modified Ruthenium Monomer Preparation

Commercially available reagents and abbreviations used for synthesizing a methacrylate-modified ruthenium monomer preparation are as follows. Hexahydrate Tris(bipyridine)ruthenium(II) dichloride, ($Ru(bpy)_3Cl_2 \cdot 6H_2O$, Strem Chemical, 98%), Anion exchange resin, DOWEX 1x8-100 (chloride form, Dow Chemical), 4,4'dimethyl-2,2'-bipyridine (Aldrich, 99%), cis-bis(bipyridine) dichlororuthenium(II) dihydrate (Aldrich, 99%), Selenium Dioxide (Aldrich, 99.8%), sodium borohydride (Aldrich, 98.5%), ammonium hexafluorophosphate (Acros, 99.5%), and methacryloyl chloride (Aldrich, 97%) are purchased.

To prepare $Ru(bpy)_2$(4-methyacryloylmethyl-4'-methylbpy)$^{+2}$ $(PF_6^-)_2$ monomer, synthesis of 4-hydroxymethyl-4'-methylbpy (**1**) is first performed by combining selenium dioxide (4.0 g, 36 mmol) and 4,4'-dimethylbpy (4.0 g, 22 mmol) in 1,4-dioxane (200 mL).[1] The reaction mixture is refluxed and stirred for 24 h. After cooling to room temperature, the mixture is filtered and concentrated to dryness. The residue is mixed with $CHCl_3$ (100 mL), filtered, and the filtrate is concentrated again. This series of steps is done two additional times (2×100 mL $CHCl_3$). Crude NMR analysis showed a 1:10:2 mixture of starting bipyridine, monooxidation and dioxidation products. This mixture (3.0 g crude) is suspended in CH_3OH (40 mL) and a solution of $NaBH_4$ (750 mg) in NaOH solution (13 mL, 0.2 M) is added drop-wise while cooling in an ice bath. The mixture is stirred for 2 h at room temperature. The reaction is filtered and the CH_3OH is removed by rotary evaporation. The aqueous residue is washed with Na_2CO_3 (saturated, 10 mL) and extracted with $CHCl_3$ (2×50 mL). $CHCl_3$ solution is dried over $MgSO_4$ then evaporated. The product is purified using column chromatography eluting with 5% CH_3OH in CH_2Cl_2, obtaining 1.9 g monomer **1** in a 44% yield.

To synthesize $[Ru(bpy)_2$(4-hydroxymethyl-4'-methylbpy)$]^{+2}$ $(PF_6^-)_2$(2)[2-3] Monomer **1** (455 mg, 2.27 mmol) is combined with cis-bis-bpy-dichloro-ruthenium(II) dihydrate (1.02 g, 1.96 mmol) in EtOH (40 mL). The mixture is refluxed for 22 h then the EtOH is removed by rotary evaporation. The red residue is dissolved in H_2O (30 mL) and NH_4PF_6 (640 mg, 4.14 mmol) is added. The mixture is stirred for 5 min then filtered and the solid is dried over P_2O_5 to obtain 1.61 g monomer **2** in a 91% yield. To prepare the product $[Ru(bpy)_2$(4-methacryloylmethyl-4'-methylbpy)$]^{2+}(PF_6^-)_2$ (**3**),[4] first monomer **2** (495 mg, 0.547 mmol) is dissolved in DMF (20 mL) and cooled to 0°C on an ice bath. Then after Et_3N (400 µL, 2.86 mmol) is added and stirred for 5 min, methacryloyl chloride (270 µL, 2.76 mmol) is added drop-wise. The reaction mixture is stirred in the dark for 24 h where it is allowed to warm to room temperature. The solution is filtered through celite with CH_2Cl_2 (40 mL) then washed 2×50 mL with 3% $NaHCO_3$ (aq.) and water (2×50 mL). The organic layer is dried with $MgSO_4$ and concentrated to about 10 mL. The red solution is then added drop-wise to Et_2O (200 mL) while stirring and the orange precipitate is collected by vacuum filtration and dried under high vacuum to yield 290 mg (55%) of monomer **3**.

S2. Underlying Polymer Chemistry and Molding Methods

S1.1. pH Response of pAA Hydrogel

The weak acid moiety of the acrylic acid (AA) monomer has a pKa=4.35 such that in neutral pH environments a high fraction of the monomer is deprotonated. With polymerization, poly-(acrylic acid) (pAA) forms anionic hydrogel networks under neutral conditions. The osmotic pressure difference that is generated by the charged polymer matrix initiates gel swelling under these conditions. Conversely, in acidic environments, a high fraction of pAA moieties are protonated, neutralizing local charge density within the hydrogel matrix and triggering pAA gel contraction as net water flow is directed into the surrounding solution.

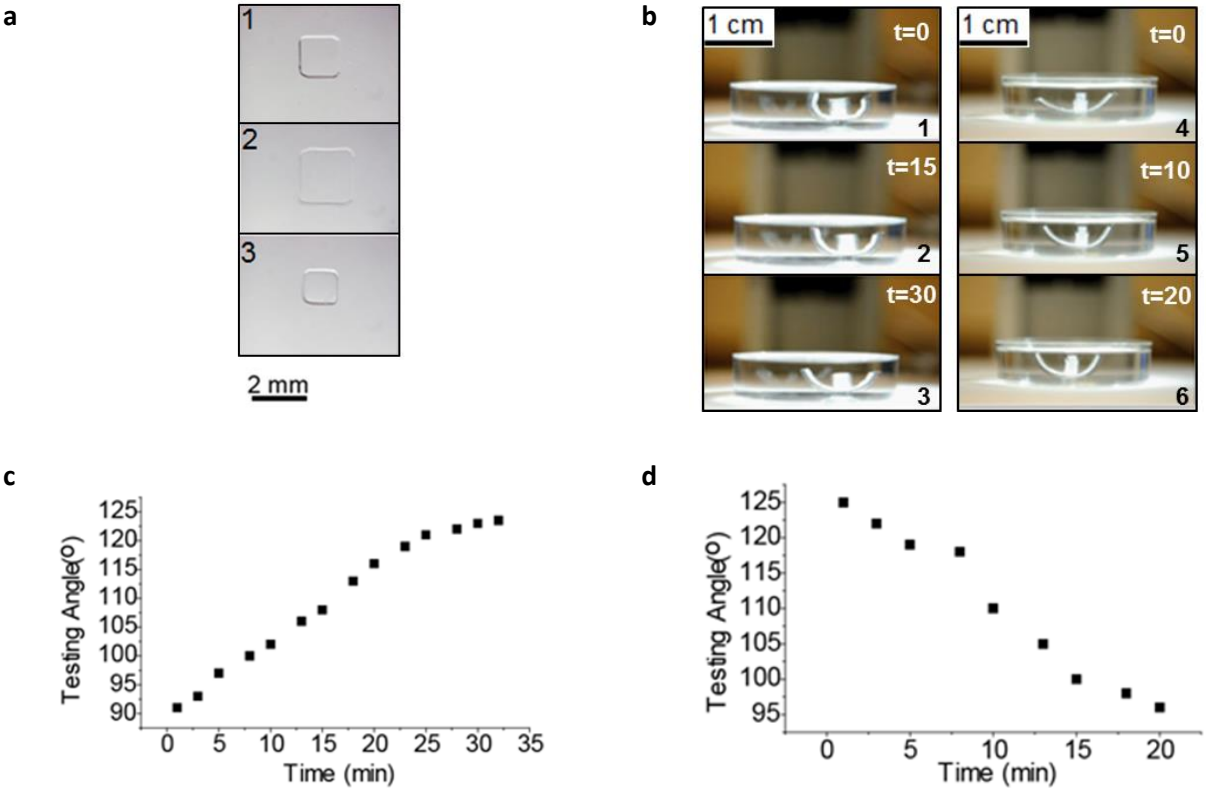

Figure S1. a) Contractile and expansive behavior of a pAA hydrogel is analyzed by measuring the lateral diagonal distance of the gel when exposed to changing pH solutions. (1) pAA hydrogel in EtOH solution shows a neutral extent of pAA swelling; (2) pAA hydrogel in pH 9.0 solution swells to approximately 120% of initial geometry; (3) pAA hydrogel in pH 2.0 solution contracts to approximately 80% of initial geometry. b) Contractile and expansive behavior of a pHEMA/pAA bimorph (unmodified gel) composite hydrogel is analyzed by measuring the device curvature angle when exposed to changing pH solutions. (b-1 to b-3) bimorph composite conformational change occurs when solution is changed from pH 9.0 to pH 2.0; (b-4 to b-6) reversion conformational change occurs when solution is changed from pH 2.0 to pH 9.0; (c) quantitative rise in curvature angle measured from 0 to 30 min of exposure to pH 2.0; (d) quantitative lowering in curvature angle measured from 0 to 20 min of exposure to pH 9.0.

Prior to incorporating our particular pAA formulation into more complex chemical systems, we analyze the specific conformational changes experienced by the hydrogel network across a range of pH values as well as the effects of polymer matrix on overall pKa behavior. In Figure S1a-1, a $2 \cdot 10^{-3}$ cm^3 pAA hydrogel network adopts what we characterize as a neutral degree of swelling when suspended in an EtOH solution immediately following curing. In Figure S1a-2, the same gel is observed to swell to approximately 120% of its original lateral diagonal dimension when placed in a pH 9.0 aqueous solution. In Figure S1a-3, the pAA gel is observed to contract to 80% of its neutral swelling state when exposed to pH 2.0 (aq). As depicted in Figure S1-b, when solution pH is gradually increased from pH 2.0 to pH 9.0, the extent of gel expansion varies sigmoidally, with the maximum degree of strain change occurring between pH values of 4-6. This analysis suggests that in order to achieve the optimal efficiency of pAA hydrogel actuation it is necessary to limit experimental pH values to within this range. Furthermore, we observe that though the apparent pKA of a pAA hydrogel network may be slightly higher than the free monomer, 4.35 remains a reasonable estimate of protonation fractions within the polymeric matrix.

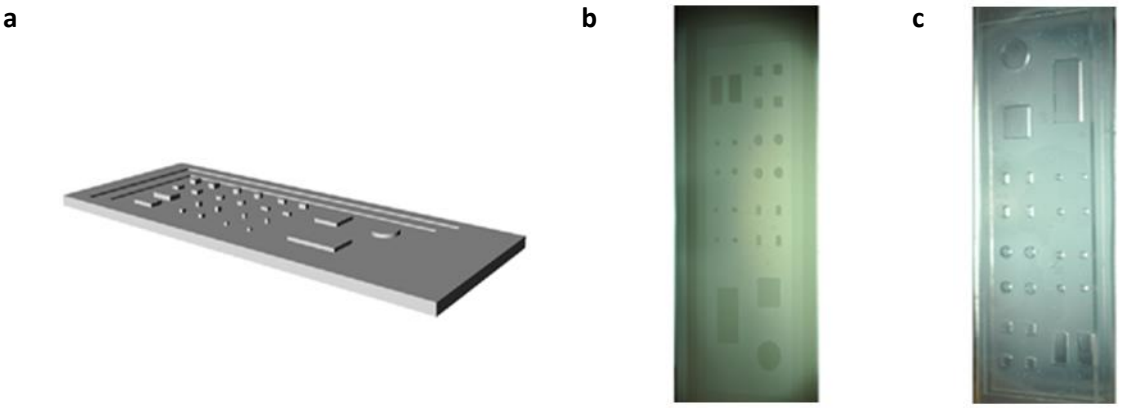

Figure S2. The fabrication of uniform RuPAA hydrogels of varying dimensions and geometry is performed with photolithographic processes. (a) 3D file used to prepare the plastic master; (b) printed plastic master; (c) silicone mold prepared from the master.

S1.2 pH Response of pHEMA/pAA Bimorph Devices

A composite hydrogel that consists of a pH-responsive actuatable sub-layer as well as an inactive hydrogel top-layer, each with a differential swelling ratio and modulus value, is a useful form factor to investigate performance constraints and capabilities of hydrogel-based actuatable devices. Figure S1b (1-3) depicts how the contraction of the pAA sub-layer yields an overall expansion of the bimorph device curvature angle as the pH is lowered from 9.0 to 2.0. Figure S1b (4-6) depict how the expansion of the pAA sub-layer yields an overall contraction of the bimorph device curvature angle as the pH is increased from pH 2.0 to pH 9.0. A quantitative assessment of how the curvature angle of the bimorph composite changes with exposure time to a pH 2.0 solution and a pH 9.0 solution are illustrated in Figure S1c and Figure S1d, respectively.

S3. Molding-Based Fabrication of Polymer Actuators

S3.1. 3D-Printing for Photolithographic Preparation of pAA Hydrogel Structures

A 3D design of a plastic mold is first simulated on Rhinoceros software (Fig. S2a). A 3D printer (Viper Stereo Lithography Apparatus) is then used to produce a plastic master (Fig. S2b). A commercial silicone Ecoflex 00-30 is used to fabricate a rubber mold (purchased from Smooth-On) from the 3D-printed plastic master. Ecoflex precursors are mixed in a ratio of 1:1 v/v, and this mixture is then poured into the plastic mold (Fig. S2c). After curing at 65°C for 15 min, the silicone rubber can be peeled away from the master and filled with pre-polymer solution. Both pAA and pHEMA gels are cured according to the same procedure, in which silicone molds are filled with pre-polymer solution and then irradiated at 298 nm UV light with 300 W for 150 sec such that the total exposure dose is approximately 1000 $mJ \cdot cm^{-2}$ (Fig. S3a). The gel structures are then removed from the mold and immersed in EtOH for 2-3 d to remove excess reagents. In the case of the composite pAA gel entrained with RuBPY and the IrO_2-PAA negative control gels, the gel is then immersed in IrO_2 NP solution overnight.

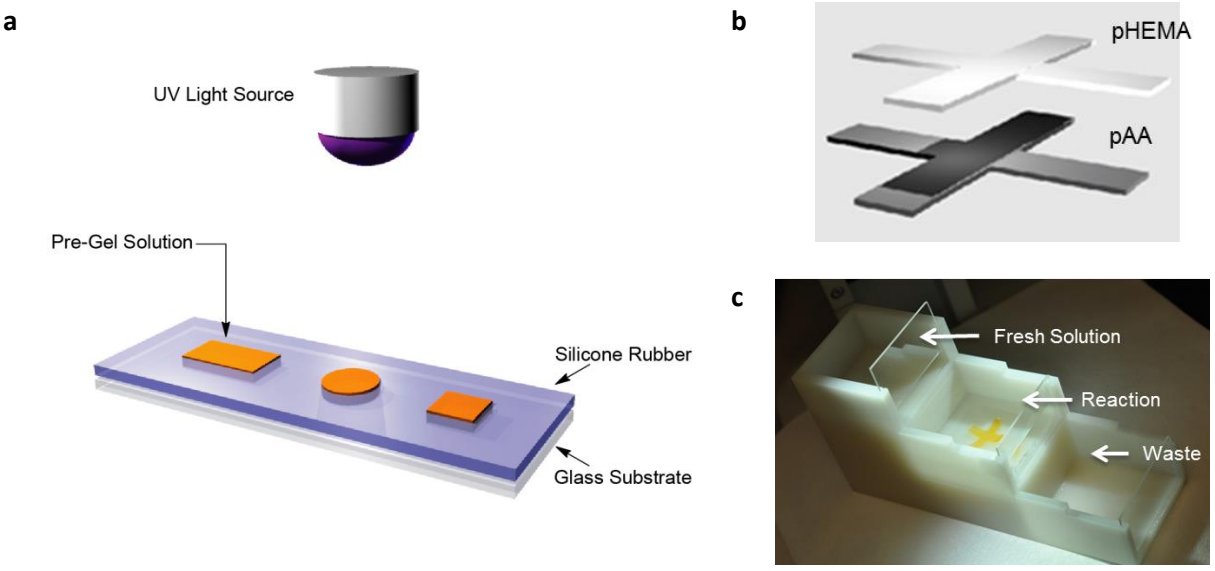

Figure S3. a) The process flow for the fabrication of pAA hydrogels and RuBPY-PAA composite gels depicts the ability to control uniform initial hydrogel geometries for inter-experimental consistency. (b) Schematic illustration of assembly of bimorph functional actuator; (c) A semi-automatic multi-cycling device with a 3-step chamber and a pHEMA/RuIrPAA bimorph actuator in the reaction chamber.

S3.2. Bimorph Preparation with pHEMA Hydrogel Top-layer

In order to fabricate a hydrogel device that can perform mechanical work, it is necessary to prepare a material interface with differential swelling behavior across the experimental pH range. pHEMA is selected as the sub-layer for the bimorph structure preparation due to its comparatively high pKa of 13.82, which lies far outside the pH window associated with water oxidation reactions. Generally, the bimorph device is fabricated by combining 6.0 g HEMA, 120 mg EGDMA, 400 mg DMPA, and 1000 mg Brij 58 to 2 mL dH_2O and pouring 2 mL of the resulting pre-polymer solution volume into a 5 cm petri

dish and irradiating with 298 nm 300W UV irradiation (600 mJ·cm^{-2}) for 90 sec.[5] The resulting pHEMA sub-layer is then covered with 2 mL of either pre-polymer PAA or RuPAA composite solutions. The entire material system is cured for another 3 min under 298 nm UV light and 300 W (1200 mJ·cm^{-2}) to fully cure both hydrogels into a bimorph structure (given schematically in Fig. S3b). A 0.61cm^3 volume of pAA composite is extracted from the bulk volume such that the volume ratio of the RuPAA bimorph component relative to the total petri dish volume is 0.111.

S3.3. 3D-Printing of Multi-Cycling Device

A 3D design of a 3-chambered multi-step solution refreshment device is first simulated on Rhinoceros software. A 3D printer (Viper Stereo Lithography Apparatus) is used to produce a plastic prototype of the intended structure (Fig. S3c). Glass slides can then be inserted between each level of the device to control timing of solution retention or removal. The highest chamber is a resource chamber that contains a pH 5.5 CO_2-saturated $Na_2S_2O_8$ solution that can flood the reaction chamber below when an intervening glass gate is removed. The bimorph gel is placed in the reaction chamber and following irradiation, the waste solution can be evacuated into the lowest waste chamber by again opening an intervening glass gate. Not only does this device facilitate more complete solution refreshment, but it also allows stationary positioning of the bimorph structure to better facilitate time-lapse imaging over multi-cycle system actuation.

S4. Quantification of IrO_2 Hydrogel Absorption

UV-Vis spectroscopy is used to detect the difference in absorption of IrO_2 NPs before and after the immersion of RuBPY-PAA composite gels. During gel immersion, the colorimetric intensity of the surrounding IrO_2 NP solution is observed to decrease concurrently with the absorptive uptake of the NPs into the gel matrix (Fig. S4). The molar ratio of each component in the RuIrPAA polymer network is calculated using their respective UV-Vis absorption ratios. According to the Beer-Lambert Law in Equation S1 and S2,

$$A_i = \varepsilon l c_i \quad \text{Eq. S1}$$

$$A_f = \varepsilon l c_f \quad \text{Eq. S2}$$

where A_i and c_i are the absorption ratio and concentration prior to gel immersion, and A_f and c_f are the absorption ratio and concentration following gel immersion, the fraction of absorbed IrO_2 NPs can be calculated as in Equation S3:

$$\frac{c_i}{c_f} = \frac{A_i}{A_f} = \frac{0.116}{0.143} = 0.81 \quad \text{Eq. S3}$$

From this we conclude that 19% of IrO_2 content was extracted from the external solution volume by absorption into the RuBPY-PAA composite network following overnight immersion. The known

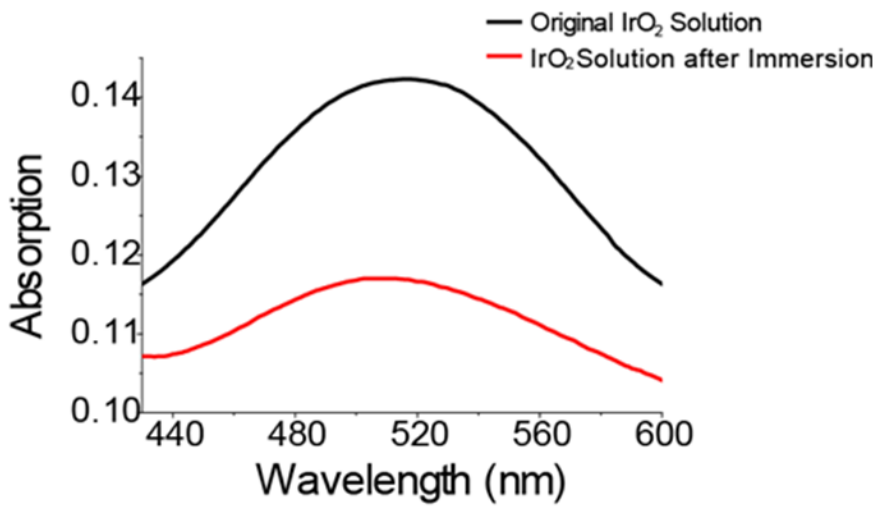

Figure S4. The UV-VIS absorbance of IrO_2 NP solutions prior to and following overnight hydration of a pAA composite gel is used to calculate the moles of IrO_2 NPs absorbed into the hydrogel matrix as well as the ratio of photosensitizer and catalytic centers within the gel.

concentration of the initial NP solution, c_i, is 0.67 mM, and the known volume, V_{Ir}, of IrO_2 NP solution used for immersion is 1 mL such that N_{Ir}, the total moles of IrO_2 in one gel of these dimensions, can be calculated as in Equation S4:

$$\begin{aligned} N_{Ir} &= C_{Ir} \times V_{Ir} \times 19\,\% \\ &= 0.67\ mmol\ /\ L \times 1mL \times 19\,\% \\ &= 1.3 \cdot 10^{-4}\ mmol \end{aligned} \qquad \text{Eq. S4}$$

Each RuIrPAA composite gel has a total volume $V_{gel} = 2 \cdot 10^{-3}$ mL. From the preparation method, each cubic centimeter of pre-gel solution contains 2.4 mmol AA and $1 \cdot 10^{-3}$ mmol RuBPY. Given the moles of AA and RuBPY known to be incorporated into the pre-polymer solution, the final mole ratios of photo-reactive components incorporated into a composite gel are $N_{AA}:N_{Ru}:N_{Ir}=24:0.001:0.64$. We conclude from this calculation that the IrO_2 NPs are present in excess of the gel-entrained RuBPY and there should be no reaction inhibition due to the absence of geometrically coordinated RuBPY-IrO_2 pairs.

S5. Experimental Controls and Procedures

S5.1 Experimental Measurements

All experiments are carried out in aqueous solution. Images of gel structures are taken with an Olympus SZX7 microscope.

S5.2. Impacts of Water Photooxidation on Ambient pH

Upon irradiation, a material system that includes the photosensitizer RuBPY, the electron acceptor $S_2O_8^{-2}$, the catalyst IrO_2, and the aqueous solution environment will rapidly react and generate an increase in universal proton concentration throughout the ambient solution. Without buffering, the pH drops precipitously until a dark green product is generated by the resulting mixture of remaining RuBPY complex and aggregated IrO_2 NPs. Previous experimental systems use buffer to maintain stable solution pH throughout the reaction and to therefore avoid NP aggregation.[6] For systems of similar design, it is expected that macroscopic length change in actuatable hydrogel geometry occurs concurrently with NP aggregation and system irreversibility. In order to create a reversible system, we prepare an experimental system that allows controlled pH decrease as photooxidation proceeds, that avoids aggregation of IrO_2 NPs by avoiding extreme pH environments, and that is capable of restoring original gel geometry after photooxidation of water ceases.

S5.3 Forms of Function for Hydrogel Devices

In order to conduct experiments concerning pH-responsive hydrogel composites that have photo-reactive elements entrained within their matrix structure, several functional hydrogel device form factors were necessary to prepare. The specific forms of function are succinctly listed below.

(A) Control pAA gel

(B) Control IrO_2-PAA gel

(C) RuIrPAA composite gels to study geometric effects of pH change

(D) pHEMA/RuIrPAA composite bilayers to study single cycle actuation

(E) pHEMA/RuIrPAA composite bilayers to study multi-cycle actuation

S5.4 Control Experiment for RuBPY-PAA Gels without IrO_2 Immersion

As shown in Figure S5a, the control group of RuBPY-PAA gels fabricated without immersion in the IrO_2 NP solution exhibit negligible dimensional change, indicating the absence of the photooxidation reaction. There is no subsequent pH value change in the environment. IrO_2 NPs are not absorbed into the gel, and RuBPY-modified acrylate monomers are not effectively absorbed by the polymer matrix within the experimental time regime.

S5.5. Control Experiment for IrO_2-PAA Hydrogels without RuBPY Entrainment

As shown in Figure S5b, unmodified pAA control gels immersed in a pH 5.5 citric acid IrO_2 NP solution exhibits no detectable pH change or change in gel length (Fig. S5c). The strain change is approximately 2.5%, which is attributed to the increase of the ionic strength of the solution with the addition of sodium persulfate.[7]

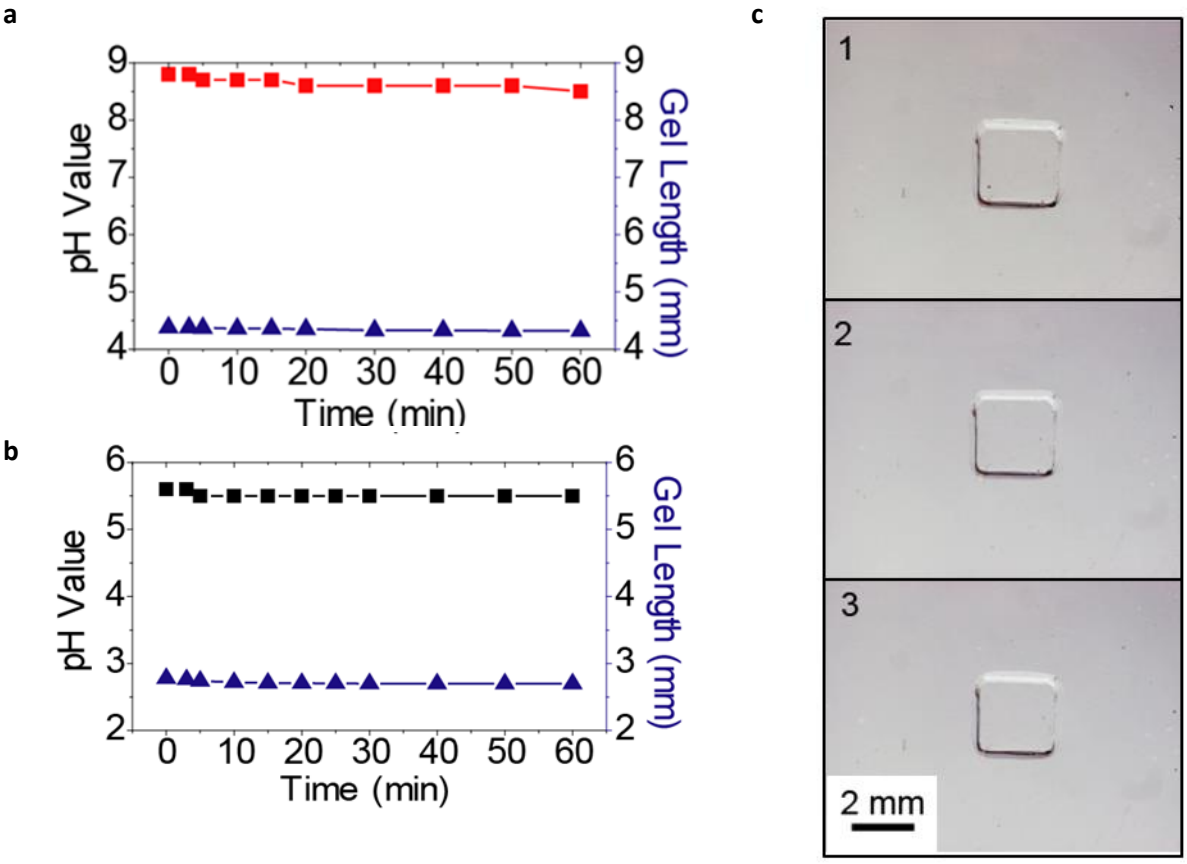

Figure S5. (a) Control experiments are performed first on RuBPY-PAA without immersion in IrO_2 NP solution prior to irradiation and measure negligible pH change and negligible gel length change over 60 min; (b) control experiments are then performed on IrO_2-PAA hydrogels (unmodified hydrogels immersed overnight in NP solution) that show the uniformity of gel size and the negligible effects of minor ionic strength increase; (c) pH values and gel length for this control experiment remain constant during the control experiments.

S5.6. Experimental Set-Up for Single Cycle Reversibility of RuIrPAA Gels

In order to observe single-cycle system reversibility, a RuBPY-PAA composite hydrogel is immersed in IrO_2 NP solution overnight to allow for uniform absorption of the IrO_2 NPs into the composite hydrogel. A volume of aqueous solution is simultaneously equilibrated with atmospheric CO_2 overnight until the solution pH reaches 5.5. Immediately prior to the experiment, the IrO_2 NP solution surrounding the pAA composite gel is replaced with the aqueous solution. 200 µL of 100 mM NaS_2O_8 are next added to the solution volume, resulting in a visible polymer contraction due to ionic strength increase. Upon

irradiation of the system, the cube of RuIrPAA gel measuring $2.0 \cdot 10^{-3}$ mm^3 begins to contract. Following 30 min of actuation however, the final pH is equilibrated at pH 4.9.

To understand the reason for the early pH equilibration, it is first necessary to further evaluate the role of CO_2 in reversible composite pAA actuation. When the gel system is moved into the dark immediately after irradiation halts, a reversion to approximately 80% of the original geometric volume is achieved after 90 min. This effect is attributed to buffering by the bicarbonate equilibrium generated by dissolved CO_2; as proton concentration in ambient solution rises, bicarbonate is converted to carbonic acid and pAA composite gel volume reverts towards its original degree of expansion.

S5.5. Control Experiment for pAA Hydrogel Irradiation in IrO_2 / RuBPY Solution

Once the cured pAA hydrogels are removed from the silicone molds, they are immersed in 3 mL of IrO_2 NP solution in a 2.5 cm diameter petri dish. Solution pH is adjusted to 8.9 by addition of 0.1 M NaOH, which causes the pAA gel to swell dramatically in the IrO_2 solution. 50 μL 6.6 mmol $[Ru(bpy)_3]Cl_2$ solution and 50 μL 100 mM $Na_2S_2O_8$ solution are added separately to the petri dish, causing an instantaneous but moderate gel volume reduction due to the increase of ionic strength in the solution. Following initiation of irradiation, water oxidation proceeds to generate a universal proton gradient that results in a pAA gel volume reduction and a strain change of up to 40% in the pAA gel.

Though final realized strain changes are significant, this system remains temporally limited due to the delayed gel contraction relative to pH change such that the system requires approximately 30 min to achieve equilibrium geometry. We note that upon reaction completion, the ambient pH drops to 2.5, which causes significant aggregation of IrO_2 NPs and system irreversibility. These results indicate that the pAA gel in the presence of RuBPY and IrO_2 has the anticipated response to the pH change caused by the water-splitting reaction. Though some asymmetry in the relative volumetric change within the actuated gels can be observed during irradiation, upon cessation of the water oxidation reaction, the structure geometries equilibrate to uniformity. Due to experimental conformational differences between experimental trials, gel dimensions are measured using the diagonal length of the surface area of the gel in order to minimize measurement subjectivity.

S6. Catalytically-Induced Proton Gradients and Irreversible Aggregation

The initial and final states of the system during irradiation, beginning at pH 5.5 and lowering to pH 5.15, yield an observable proton concentration change of $3.92 \cdot 10^{-6}$ M that corresponds to the minimum theoretical quantity of protons produced. However, it is also necessary to consider the proton uptake by the carbonic acid equilibrium and by the acrylic acid functional groups during this state change to better approximate catalytic performance during bimorph irradiation. To calculate theoretical proton abstraction by the carbonic acid equilibrium, the total concentration of available CO_3^{-2} is calculated as $2.58 \cdot 10^{-5}$ M and the Henderson-Hasselbalch relationship is used to calculate a $[A^-]/[HA]$ ratio of 0.135 at pH 5.5 and 0.060 at pH 5.15. This corresponds to a total of $1.60 \cdot 10^{-6}$ M protons abstracted from solution as the carbonic acid equilibrium shifts to the left.

An identical calculation is performed for the acrylic acid functional groups present in the bimorph reaction solution. $[A^-]/[HA]$ ratios for the initial and final system states are determined to be 14.12 and

6.31, respectively. If the concentration of acrylic acid present in the environment is calculated using total reaction volume, there exists a theoretical concentration of $1.81 \cdot 10^{-1}$ M acrylic acid available for

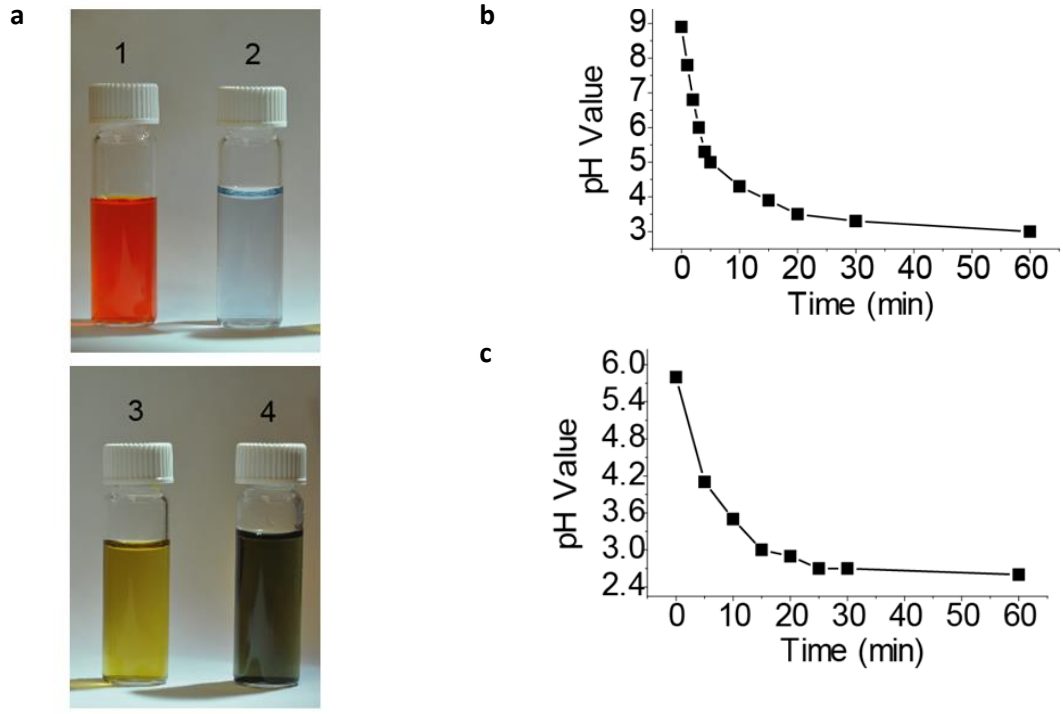

Figure S6. The photooxidation reaction proceeds without any buffering moieties. (a-1) 1.0×10^{-4} M $Ru(bpy)_3^{2+}$ solution; (a-2) 6.0×10^{-4} M IrO_2 NP solution; (a-3) 1.0×10^{-2} M $Na_2S_2O_8$ is combined with all reagents; (a-4) Following irradiation without buffering, IrO_2 NPs irreversibly aggregate in solution; (b) The profile of pH value change with initial solution pH=8.9; (c) The profile of pH value change with initial solution pH=5.6.

protonation. This yields a total proton abstraction due to this equilibrium of $1.28 \cdot 10^{-2}$ M as pH lowers from 5.5 to 5.15. The maximum concentration of protons produced by the catalytic cycle is therefore $1.28 \cdot 10^{-2}$ M. The inclusion of proton abstraction by the carbonic acid equilibrium and the proton concentration in solution are orders of magnitude smaller and contribute negligibly to the final abstracted proton concentration.

The ratio of $S_2O_8^{-2}$ consumed relative to protons produced is 1:2 such that $1.92 \cdot 10^{-5}$ moles of $S_2O_8^{-2}$ are necessary to achieve the total proton flux due to irradiation of the bimorph system. Under the assumption that catalytic degradation is the limiting reagent within the system, a final pH of 5.15 equates to a 95.8% reaction conversion of the $S_2O_8^{-2}$ reagent. This point is in such close proximity to the complete reaction of $S_2O_8^{-2}$ that the bimorph reaction system could not achieve pH 5.10 due to the prior total elimination of electron acceptor. The difference in these two values is on the order of pH measurement accuracy, and it is improbable that catalytic degradation occurred concurrently with the complete reaction of electron acceptor.

To further confirm that $S_2O_8^{-2}$ is the limiting reagent, the dynamics of the catalytic system are analyzed by combining the RuBPY solution, the electron acceptor $S_2O_8^{-2}$, and IrO_2 NPs in the same quantities and concentrations as are present within the typical bimorph experimental system. The

bimorph structure and therefore the acrylic acid functional groups that provide the vast majority of the proton sink during irradiation experiments are excluded from the solution. In the case where 0.1 M NaOH is added to the solution such that the initial pH=8.9, the final solution following 60 min of irradiation equilibrates at pH 2.6. It is at this point that the significant drop in system pH causes an asymptotic slowing of pH change as well as the development of a distinctive dark green solution color resulting from the mixture of remaining RuBPY complex and aggregated IrO_2 NPs (Fig. S6a-b). Catalytic inactivation of the system is clearly present; if the $S_2O_8^{-2}$ in solution is allowed to react to completion, the expected final pH would be 1.88.

A very similar case is observed when the solution is equilibrated with atmospheric carbon dioxide such that the initial pH is 5.5 as in a typical bimorph experiment (Fig. 6c). When irradiated for an hour, experimental pH for this solution again lowers to 2.6 and the theoretical pH value remains 1.88 due to the relatively small quantity of proton abstraction via the carbonic acid equilibrium. Following from these calculations, we conclude that it is the persulfate and neither the photosensitizer nor the catalyst within the system that is the source of the equilibration of experimental trials between 5.1 and 5.15.

In the case of the bimorph system, moderate pH change is intended in order to induce macroscopic volume change of the pAA-based materials. When the bimorph is present, due to effective pH buffering contribution of the acrylic acid moieties, the complete reaction of $2.0 \cdot 10^{-5}$ mol $S_2O_8^{-2}$ yields a TON value of 87.1. Without the buffering capability of the acrylic acid, the precipitous pH decline and subsequent NP aggregation reduces the fraction of reacted $S_2O_8^{-2}$ to 0.188 and the TON value to 70.7. In practice, the persulfate reagent can be readily refreshed and its quantities readily altered in order to control intended outcomes and reversibility of the bimorph hydrogel system.

S7. Bimorph Composition and Solution Conditions at pH 5.5

The acrylic acid pre-polymer solution consists of 350 mg of acrylic acid, 11.2 mg of MBAm crosslinker, and 2 mg of RuBPY that are added to 2 mL of 1:1 H_2O:DMSO solvent and injected into a glass petri dish of 2.5 cm radius that already contains a cured layer of pHEMA gel. The resulting cured acrylic acid volume is therefore 5.5 cm^3. Upon UV curing, a pHEMA/RuIrPAA structure is extracted from the cured polymer disc that contains a total gel volume of 0.61cm^3. The volume fraction of the bimorph relative to initial reagents yields an experimental bimorph system that incorporates $5.42 \cdot 10^{-4}$ mol of acrylic acid moieties. Concurrently, adjusted quantities of MBAm and RuBPY in a given experimental system are $8.10 \cdot 10^{-6}$ mol and $2.30 \cdot 10^{-7}$ mol, respectively. $4.0 \cdot 10^{-5}$ mol of IrO_2 NPs are incorporated into the experimental system by absorption by the bimorph gels. The bimorph is next suspended in 2.8 mL of dH_2O, to which 200 µL of 100 mM $S_2O_8^{-2}$ are added for a total reaction volume of 3 mL and a final $S_2O_8^{-2}$ concentration of $6.67 \cdot 10^{-3}$ M. Regardless of the final polymer disc thickness approximation, the fraction of utilized acrylic acid moieties is a constant that is constrained by the assumed equivalent thickness of the total cured disc volume. With bubbling CO_2 through the solution overnight, the pH is lowered to 5.5 due to the presence of the carbonic acid equilibrium. Accounting for the auto-ionization of water at pH 7 and an H_2CO_3 pK_a of 6.37, the HCO_3^{-1} concentration at pH 5.5 in a 3 mL solution volume is $3.06 \cdot 10^{-6}$ M and the H_2CO_3 concentration at pH 5.5 is $2.27 \cdot 10^{-5}$ M.

S8. Mechanisms of Single Cycle System Reversibility for Bimorph Composite

When the bimorph undergoes irradiation via the 3-chambered solution exchange, the $S_2O_8^{-2}$ in solution limits the extent of reaction and therefore the final pH according to the overall process of the photo-oxidation reaction as shown in Equation S5:

$$H_2O\ (l) + S_2O_8^{-2}(aq) \xrightarrow{h\nu,[Ru(bpy)_3]^{+2},IrO_2} 2H^+(aq) + 2SO_4^{-2}(aq) + 2e^- \qquad \text{Eq. S5}$$

In our previous calculation, the Henderson-Hasselbalch is used to approximate steady-state total proton abstraction during the irradiation portion of the reaction, further assuming that the carbonic acid equilibrium is synchronous with $S_2O_8^{-2}$ consumption. In practice, the carbonic acid equilibrium lags behind the pH gradient that is generated inside the hydrogel structure such that upon completion of irradiation, the carbonic acid has not yet reestablished equilibrium. Because the order of abstraction magnitude contributed by the carbonic acid equilibrium is negligible compared to proton abstraction by the pAA hydrogel, this difference has no bearing on the question of whether $S_2O_8^{-2}$ is entirely consumed during an irradiation cycle of the bimorph structure. Observationally, there is use in assuming that upon complete reaction of $S_2O_8^{-2}$ and cessation of irradiation, an instantaneous proton flux is introduced into the system. The imbalance of protons relative to HCO_3^{-1} ions in solution forces the carbonic acid equilibrium left, as shown in Equation S6:

$$H_2CO_3(aq) \leftrightarrow H^+\ (aq) + HCO_3^{-1}(aq) \qquad \text{Eq. S6}$$

Assuming again that the pH of the solution is initially 5.5, $[HCO_3^{-1}] = 1{\cdot}10^{-5.51}$ M, and $[H_2CO_3] = 1{\cdot}10^{-4.64}$ M, if sufficient protons are instantaneously added for system pH to achieve 5.15, solution equilibration will proceed until $[HCO_3^{-1}] = 1{\cdot}10^{-5.75}$ M. It is during this transitional period that pH of the system rises to pH 5.24 and concurrent pAA deprotonation reduces the bimorph curvature angle and radius of curvature—achieving reversibility as the bimorph approaches its initial geometry. The cooperativity of these two processes serves to further accentuate the transition; as more protons are liberated from acrylic acid moieties within the gel, they fractionally lower the pH and force the carbonic acid equilibrium expression further left. Theoretically, this effect could proceed until all bicarbonate present in solution is consumed. To achieve reversibility, it is therefore crucial to tune the quantity of persulfate in the system relative to AA moiety concentration. If final pH values appreciably lower than 5.1 are reached during irradiation of the bimorph composite, the excess quantity of protons rapidly overpowers neutralizing effects of bicarbonate ions in solution. Though equilibrium would re-establish following identical mechanisms, no conformational change would be evident in the bimorph because all bicarbonate is converted to carbonic acid with little to no visible pH change. When the ambient solution remains unrefreshed following the irradiation cycle, a complete return to the previous gel conformation is not observed because the net proton production exceeds the buffering capacity of the bicarbonate by several orders of magnitude.

S9. Mechanisms of Multi-Cycle Reversibility

S9.1 Influence of Ionic Strength

In order to achieve complete reversibility across multiple cycles, the bicarbonate alone is insufficient. Furthermore, the complete reaction of persulfate during a single irradiation cycle deprives the solution of sacrificial electron acceptor. For these reasons, the solution must be refreshed via a multi-chambered mechanism immediately following reaction cessation to achieve complete geometric reversion. Upon refreshment, the bimorph is observed to undergo an immediate (though gradual) transformation that concludes when the bimorph achieves its initial curvature angle and conformation. It is reasoned that because each reaction inputs a particular quantity of protons into the bimorph and surrounding solution, and the complete reaction of persulfate exceeds the buffering capacity of the bicarbonate equilibrium, it is impossible for the bimorph to achieve full reversibility from the effects of deprotonation alone.

During irradiation, the ionic strength of the solution surrounding the bimorph hydrogel increases from $2.0 \cdot 10^{-2}$ M to $3.2 \cdot 10^{-2}$ M as the pH changes from 5.5 to 5.15, which is known to directly affect the swelling volume of pAA. The observable mechanical change is therefore a composite effect of both protonation fraction increase within the pHEMA/RuIrPAA gel and the higher ion concentration in the surrounding solution. When the surrounding solution volume is extracted following irradiation and immediately replaced with a low ionic strength solution, the osmotic pressure differential drives water into the gel until the distinct swelling ratios native to the pAA and pHEMA hydrogels as well as the mechanical resistance from the higher modulus of the pHEMA prevents further contact angle reduction. At pH 5.5, if solution ionic strength is not considered negligible relative to the concentration of gel functional group moieties, the elastic chemical potential and the chemical potential of mixing present within the hydrogel resist the influx of water such that the ionic chemical potential difference between the external solution).[8-9] At pH 5.15, the chemical potential difference falls, consistent with a pAA gel network with concurrent charge density reduction in the bimorph and ionic strengthening in the supernatant solution. When the solution is refreshed, if pH is assumed to remain approximately constant, the loss in supernatant ionic strength yields a reversion chemical potential difference that corresponds to a positive influx of water into the pAA gel and is consistent with experimental observations.

S9.2 Photosensitizer Degradation

Finally, we address the reduction of maximum bimorph actuation following multiple cycles, despite the refreshment of ambient solution and the provision of more $S_2O_8^{-2}$ reagent for each irradiation cycle. Despite the favorability of the system reversibility, after only 5 cycles the magnitude of the curvature angle change is reduced by half of first cycle performance. This is attributable to the non-ideality of the RuBPY photosensitizer, which undergoes photodecomposition and depletes the pAA gel of the Ru(II) metallocenters necessary for catalytic turnover. The degree of photosensitizer degradation evident in the relatively large bimorph volume upon multi-cycles is suggested as further evidence for the distinction between the mechanism for experimental pH equilibration for the bimorph ($S_2O_8^{-2}$ as a limiting reagent) and for the small volume RuBPY-PAA gel (photosensitizer degradation). For the multi-cycle bimorph, further experiments are needed to determine whether the same actuation extent can

still be achieved if longer irradiation intervals are used for successive cycles, or if reduction of excess photonic energy can extend the lifetime of the gel-entrained RuBPY photosensitizer.

S10. Mechanical Bending of Bimorph System

S10.1 Mechanical Analysis of Hydrogels

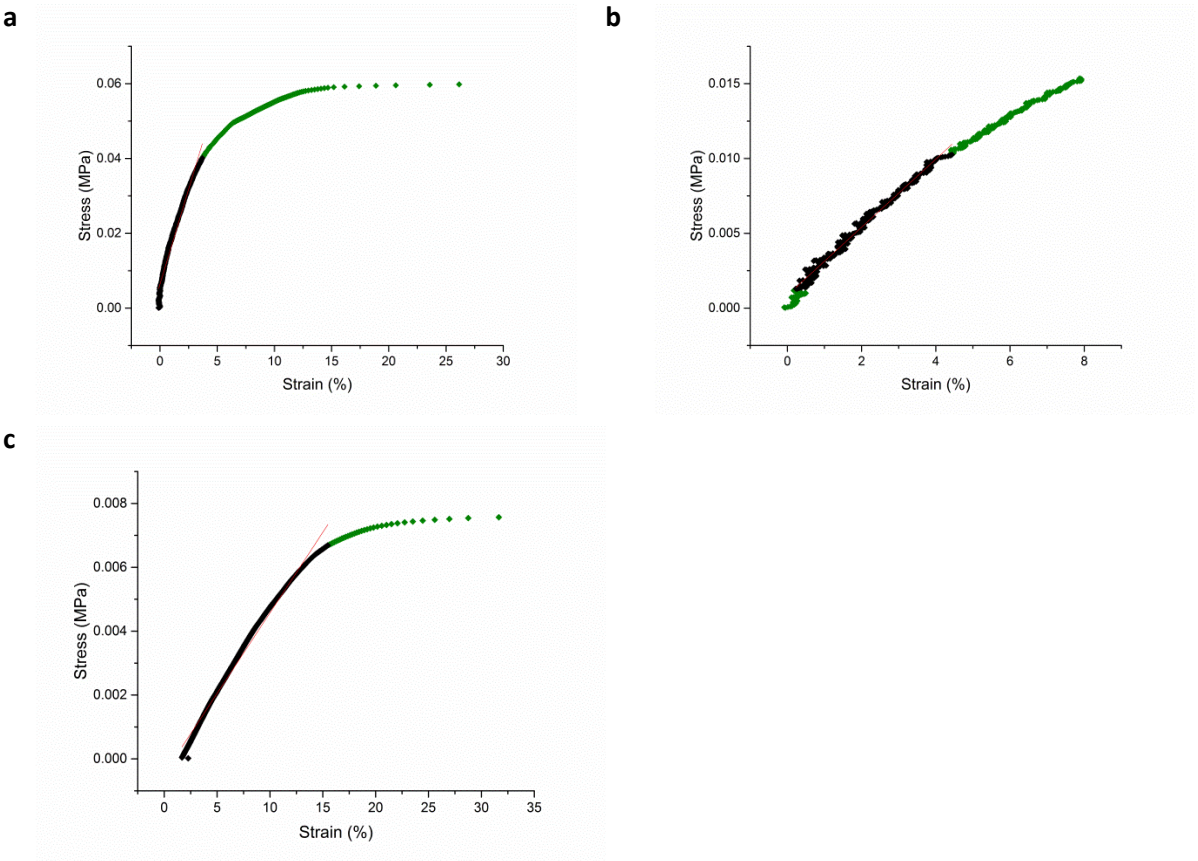

Figure S7. (a) Stress-Strain DMA measurement example of pHEMA hydrogel samples yields a relatively high Young's modulus value for pHEMA, (b) an intermediate modulus for the bimorph composite, and (c) a low modulus for pAA.

When analyzing the change in system energy within the bimorph it is first necessary to characterize the mechanical properties of the relevant hydrogels. To do so, a bimorph sample is prepared as previously described by addition of 2 mL of each pre-polymer solution into a glass petri dish with a 2.5 cm radius with sequential curing and consistent irradiation times. Separate samples of pAA and pHEMA are also prepared by curing 2 mL of each pre-polymer solution in separate petri dishes. Rectangular samples extracted from these thin polymer layers are hydrated for 72 h prior to mechanical analysis. A Q800-DMA tension clamp mount is used to perform all measurements immediately following hydrogel removal from the hydration solution. At minimum three distinct measurements are performed on each hydrogel type, yielding stress-strain curves from which elastic moduli can be calculated as tangents to

the linear portion of the curve (Fig. S7a). pHEMA exhibits the highest elastic modulus of 997±190 kPa. The average bimorph sample's elastic modulus is intermediate to these values at 251±69 kPa (Fig. S7b). The pAA has the lowest elastic modulus of 51.6±1.7 kPa (Fig. S7c) It is noted that the comparatively low elastic modulus of these samples contributes to initial noise in some stress-strain measurements that is attributed to incomplete extension of the solids even after initial force is applied. However, material attributes of all three sample types are such that the measured dimensions are rigorously upheld during the crucial intermediate portion of the stress-strain measurements. Reasonable approximations of Poisson's Ratios for each of these hydrogels are determined from the literature to be 0.43.

S10.2 System Energies of Directional Deformation in pHEMA/RuIrPAA Gel

a

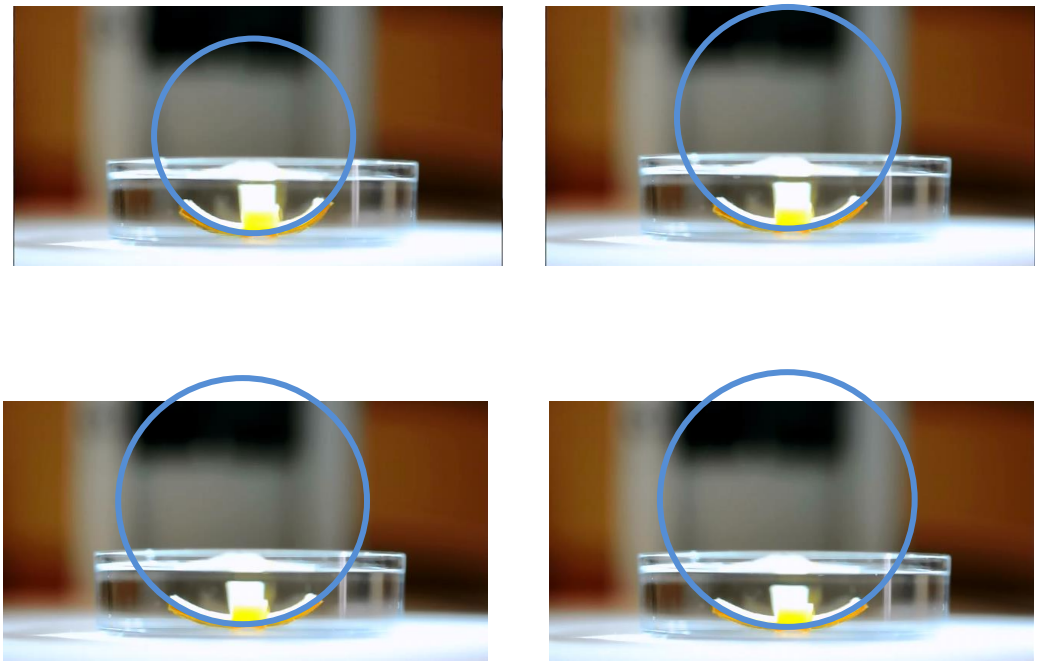

Figure S8. Curvature radius measurements for mechanical measurements on bimorph devices. Time 0 (upper left), time 12 min (upper right), time 24 min (lower left), time 30 min (lower right).

The cross-sectional profile of the bimorph is imaged during irradiation experiments and snap-shots of bimorph conformational states at 0 sec, $7.2 \cdot 10^2$ sec, $1.44 \cdot 10^3$ sec, and $1.8 \cdot 10^3$ sec irradiation times are digitally inscribed in a circle of equivalent curvature radius to the pAA layers of bimorph structure (Fig S8). Measurements are scaled with the known diameter of the petri dish from all experiments in order to determine the radius of curvature for each experimental time-point. Using a cross-shaped mechanical model to simulate the bending properties of the bimorph structure, the system energy change due to the pH gradient S_e is calculated according to Equations 1-4. In its initial state, suspended in aqueous solution, the bimorph structure adopts a minimum radius of curvature due to the difference in swelling ratios between the RuIrPAA and the pHEMA hydrogel sub-layers. As irradiation proceeds and ambient proton concentration increases, the mechanical shrinkage of the RuIrPAA composite matrix leads to expansion of the bimorph curvature radius. It is an assumption of this model that the mechanics of the

bimorph are linear such that bending and un-bending processes exhibit symmetric energy change, leading to an absolute difference of 0.464 mJ between the initial energetic state of the bimorph and the final energetic state following 1800 sec (30 min) of irradiation (Fig. S8, lower right).

S11. Reaction Efficiency

Due to the geometry of the bimorph structure, a total surface area of irradiation is calculated to be 2.19 cm^2. A 150 W lamp is used during bimorph irradiation, with an approximate irradiated area of 19.6 cm^2 and an irradiation time of 1800 sec. Irradiation density is 7.64 $J \cdot cm^{-2} sec^{-1}$ for a given experimental cycle of 30.1 kJ, far in excess of the energy use anticipated by the conformational change of bimorph structure. The efficiency of mechanical change within the system relative to this value is $1.5 \cdot 10^{-6}$ %.

To calculate the relative proportion of energy utilized by the catalytic cycle, the known quantity of protons produced during a single irradiation cycle is converted to the number of photons utilized during the reaction. RuBPY complexes are known to absorb incident photons at 450 nm, with a RuBPY→$RuBPY^*$ excitation transition of 266 $kJ \cdot mol^{-1}$. The total photon energy used by the system is therefore $10.2 \cdot 10^{-3}$ kJ, assuming 95.8% $S_2O_8^{-2}$ reagent depletion.

The thermodynamic contribution of the RuBPY complex and the $S_2O_8^{-2}$ reagent are next considered separately, with the free energy of the RuBPY complex photo-excitative cycle equal to 0 kJ and the standard state reduction potential of $S_2O_8^{-2}$ corresponding to a free energy change of $-7.76 \cdot 10^{-3}$ kJ. The thermodynamic contribution from water hydrolysis equals $4.33 \cdot 10^{-3}$ kJ. $\Delta G°_{rxn}$ is therefore -83.9 $kJ \cdot mol^{-1}$ proton produced, and total reaction free energy is $-3.22 \cdot 10^{-3}$ kJ. When the photonic energy input is also considered, a single bimorph actuation cycle requires only $6.97 \cdot 10^{-3}$ kJ—0.02% of the energy applied in the described experiments—to function. Updating the consideration of efficiency with these values yields a value of $6.7 \cdot 10^{-3}$%.

S12. References

1 P. G. Hoertz, Y.-I. Kim, W. J. Youngblood, T. E. Mallouk, *The Journal of Physical Chemistry B* **2007**, *111*, 6845.

2 L. Geren, S. Hahm, B. Durham, F. Millett, *Biochemistry* **1991**, *30*, 9450.

3 K. E. Berg, A. Tran, M. K. Raymond, M. Abrahamsson, J. Wolny, S. Redon, M. Andersson, L. Sun, S. Styring, L. Hammarström, *Eur. J. Inorg. Chem.* **2001**, *2001*, 1019.

4 S. Laib, M. Petit, E. Bodio, A. Fatimi, P. Weiss, B. Bujoli, *Comptes Rendus Chimie* **2008**, *11*, 641.

5 N. H. Mack, J. W. Wackerly, V. Malyarchuk, J. A. Rogers, J. S. Moore, R. G. Nuzzo, *Nano Lett.* **2007**, *7*, 733.

6 A. Harriman, I. J. Pickering, J. M. Thomas, P. A. Christensen, *Journal of the Chemical Society, Faraday Transactions 1: Physical Chemistry in Condensed Phases* **1988**, *84*, 2795.

7 G. M. Eichenbaum, P. F. Kiser, S. A. Simon, D. Needham, *Macromolecules* **1998**, *31*, 5084.

8 L. Brannon-Peppas, N. A. Peppas, *Polym. Bull.* **1988**, *20*, 285.

9 L. Brannon-Peppas, N. A. Peppas, *Biomaterials* **1990**, *11*, 635.